Postprint

This is the author's version of a work that was accepted for publication in *Science of the Total Environment* in 2019.
The final version was published in *Science of the Total Environment* as:
**Pieren, R., Bertsch, L., Lauper, D., & Schäffer, B. (2019). Improving future low-noise aircraft technologies using experimental perception-based evaluation of synthetic flyovers. *Science of the Total Environment*, *692*, 68-81.**
https://doi.org/10.1016/j.scitotenv.2019.07.253

# Improving future low-noise aircraft technologies using experimental perception-based evaluation of synthetic flyovers

Reto Pieren[a,*], Lothar Bertsch[b], Demian Lauper[a], Beat Schäffer[a]

[a]*Empa, Swiss Federal Laboratories for Materials Science and Technology, 8600 Dübendorf, Switzerland*
[b]*German Aerospace Center (DLR), 37073 Göttingen, Germany*

**Highlights**

- A comprehensive approach to reduce aircraft noise annoyance is proposed.
- Perception-based evaluation of future low-noise aircraft technologies is affirmed.
- Combined optimization of air vehicles and flight procedures is most beneficial.
- Reliable optimization requires consideration of several receiver locations.

**Graphical Abstract**

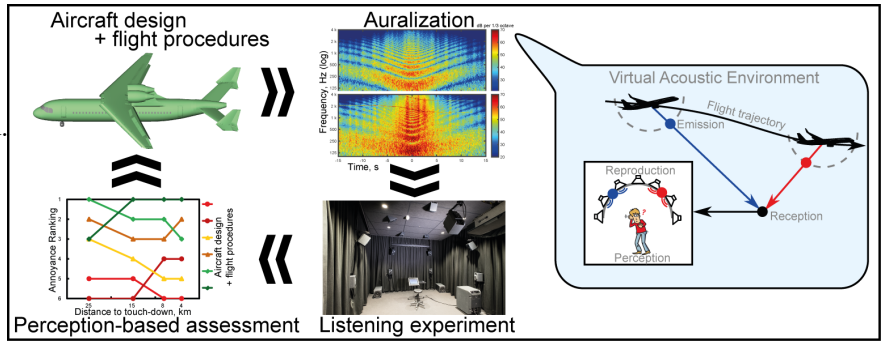


**Abstract**

Residents living in the vicinity of airports are exposed to noise from departing and approaching aircraft. Noise may be reduced by introducing novel aircraft technologies into vehicle retrofit, aircraft design and flight procedures. Nowadays, noise assessment and communication of noise are accomplished using conventional noise indicators that consider neither the perception of sound, nor its health effects. To overcome these limitations, this article presents a more comprehensive approach that supports the movement for perception-influenced design in order to reduce the negative environmental impacts and adverse health effects caused by increased air traffic noise. By means of auralization (the acoustical counterpart of visualization), possible future changes can be evaluated by considering the human perception of sound. In this study, in a virtual acoustic environment flyovers of different aircraft types and flight procedures are auralized for ground-based receiver locations, and subsequently evaluated in a psychoacoustic laboratory experiment with respect to short-term noise annoyance. Flight approaches of an existing reference aircraft, a possible low-noise retrofitted vehicle and a future low-noise vehicle design were simulated along standard and tailored flight procedures. To create realistic listening experiences of synthetic flyovers, auralization technologies were further developed regarding source synthesis, transitions between aircraft conditions, sound propagation effects and immersive sound reproduction. Listening experiments revealed significant annoyance reductions for low-noise aircraft types and tailored flight procedures, and that maximum benefit is achieved by the combined optimization of aircraft design and flight procedure. Further, it is shown that spatially distributed receivers need to be considered for a reliable low-noise aircraft technology evaluation. The reduction potential in terms of perceived noise by retrofitting current vehicles and designing new vehicle architectures is thus demonstrated. These findings suggest applying the proposed comprehensive approach to effectively reduce the impact of perceived air traffic noise in the future.

*Keywords:* Technology assessment, Aircraft noise, Simulation, Auralization, Perception

## 1. Introduction

Air traffic entails environmental impacts such as air pollution and noise. Worldwide, aircraft noise affects millions of people (e.g., (World Health Organization (WHO), 2018)). Particularly residents living in the vicinity of airports are confronted with noise from departing and approaching aircraft. Among others, they cause noise-induced sleep disturbance (Basner, et al., 2014) and noise annoyance (Guski, Schreckenberg, & Schuemer, 2017), which both may lead to negative

* Corresponding author.
*E-mail address:* reto.pieren@empa.ch.

long-term health effects (World Health Organization (WHO), 2018). Expected growth of the population, the number of passengers and the number of aircraft movements will further aggravate the problem in the future.

To counteract this tendency, the International Civil Aviation Organization (ICAO) published the "Balanced Approach" (ICAO, International Civil Aviation Organization, 2008) according to which aircraft noise management should be addressed with four principal elements that are (i) noise reduction at the source, (ii) land-use planning and management, (iii) noise abatement operational procedures, and (iv) operating restrictions. These elements are typically treated by considering conventional noise indicators, such as the equivalent continuous sound level, Leq, or the day–evening–night noise level, Lden, which are commonly used for noise assessment (Kephalopoulos, Paviotti, Anfosso-Lédée, & Van Maercke, 2014) and by airports to communicate noise information to the public (Gasco, Asensio, & de Arcas, 2017). Such indicators describe sound exposure in a generalized and highly averaged way. Evaluating the above elements on that basis neither considers the perception of sound, nor its effects. It is therefore questionable to only use such conventional indicators in noise abatement, as indicated in an aircraft noise field study on noise annoyance (Bartels, Márki, & Müller, 2015).

In the past decades, much progress has been made in the development of software tools for aircraft design and noise prediction (e.g., (Bertsch, 2013)). With noise getting more into the focus, these tools are more and more used for digital prototyping of low-noise aircraft technologies. In the perspective of single flight events, the two technical elements of the "Balanced Approach" can simultaneously be considered, namely, noise measures at the source (i) and low-noise flight procedures (iii). Current prediction software frameworks describe the noise emission of an aircraft by partial sound sources. They consider the propulsion system and the aeroacoustics of the airframe and allow calculations in relatively fine temporal, spatial and spectral resolutions, e.g. Aircraft Noise Prediction Program 2 (ANOPP2) (Lopes & Burley, 2011) or the Parametric Aircraft Noise Analysis Module (PANAM) (Bertsch, 2013).

Furthermore, in the past years considerable scientific progress has been made in the auralization of environmental acoustical sceneries. A good overview of auralization is given by (Vorländer, 2008). Analogous to visualization, this technique allows creating virtual realities that offer listening experiences of situations that do not necessarily exist in reality. Parametric calculation models to auralize the major environmental noise sources are now available, including wind turbine noise (Heutschi, et al., 2014; Pieren, Heutschi, Müller, Manyoky, & Eggenschwiler, 2014), road traffic noise (Jagla, Maillard, & Martin, 2012; Pieren, Bütler, & Heutschi, 2016), railway noise (Pieren, Heutschi, Wunderli, Snellen, & Simons, 2017), and jet aircraft noise (Arntzen & Simons, Modeling and synthesis of aircraft flyover noise, 2014; Rizzi, Aumann, Lopes, & Burley, 2014; Sahai, et al., 2016). These calculation models are physics-based and are able to create plausible listening experiences. A major achievement is that the resulting sounds are fully synthesized without the need of sound recordings. This allows listening to arbitrarily composed future scenes which was not possible before.

The combination of these two methodologies, aircraft design with noise prediction and auralization, thus enables listening to possible future aircraft technologies. This includes changes of partial sources as well as flight procedures. Such a simulation of the audible impression of novel technologies can be used for communication, assessment and evaluation purposes. The concept of using such an evaluation as a feedback to the aircraft design stage was recently coined "perception-influenced design" (Rizzi, 2016; Rizzi, Aumann, Lopes, & Burley, 2014). This idea is already well-established with sound design of passenger cars (Zeller, 2012). In contrast, first applications towards this concept in the aircraft noise sector were done only recently, e.g. by (Arntzen, Bertsch, & Simons, 2015) and (Rizzi & Christian, 2016). (Arntzen, Bertsch, & Simons, 2015) concluded that auralization is a valuable tool to support aircraft designers. (Rizzi & Christian, 2016) found that a low-noise design, as expressed by level reduction, does not equate with a low-annoyance design. This shows that the current development process of low-noise aircraft technologies that are optimized regarding classical acoustical metrics, neglecting human perception, is limited to minimize noise annoyance. However, the feasibility of the concept still needs to be demonstrated with more studies and in a broader context.

The objective of this study is to demonstrate the feasibility of a perception-based evaluation of future low-noise aircraft technologies, i.e., including novel aircraft design, retrofitting of existing vehicles, and advanced flight procedures. To that aim, different civil aircraft and flight procedures are simulated and evaluated with respect to the endpoint short-term noise annoyance, as a proxy for community noise annoyance as observed in the field. A case study is designed to evaluate the potential of air vehicle retrofitting, novel aircraft designs, and tailored flight procedures to reduce noise annoyance. This requires developing a comprehensive, multidisciplinary methodological approach, i.e. considering vehicle design, flight performance, acoustics, signal processing and human perception. To our knowledge, this is the first study that includes a perception-based evaluation of different low-noise aircraft technology levels in combination with different flight procedures.

The paper is structured as follows: Section 2 describes the simulation process and explains how different aircraft and procedures are designed, how their noise emission is predicted, how virtual flyovers are auralized for receiver positions near the ground, and how the flyovers are evaluated by human listeners to assess the design variants. It gives an overview of the process but also explains technical details where new challenges were discovered and solved. Sections 3 and 4 are dedicated to an application study for the developed methodology to answer some relevant questions about low-noise aircraft technologies. Conclusions are given in Section 5.

## 2. Methodology

### *2.1. Perception-based evaluation process – overview*

Figure 2.1 illustrates the concept of the simulation process with different modules and feedback loops developed here. The process starts with the Top Level Aircraft Requirements (TLAR) and passes through aircraft design (vehicle and procedure), componential noise emission prediction, auralization, and listening experiments with human listeners (usually

referred to as subjects) to obtain a perception-based assessment. This output is used as feedback for model improvements and/or optimization of aircraft technologies. The principles of the modules are elucidated in the following sections.

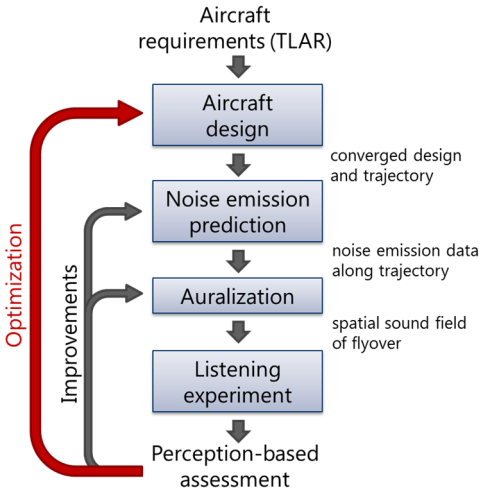


Figure 2.1. Block diagram of the simulation process for an experimental perception-based assessment and optimization of future low-noise aircraft technologies (TLAR = Top Level Aircraft Requirements).

### *2.2. Aircraft design and flight simulation*

As a first step, aircraft and flight procedures are conceived in the conceptual aircraft design process (Bertsch, 2013; Pott-Pollenske, Wild, & Bertsch, 2014; Bertsch, Heinze, & Lummer, Application of an Aircraft Design-To-Noise Simulation Process, 2014). Air vehicles are designed for a TLAR (defining parameters such as mission range and passenger numbers) with software frameworks such as Preliminary Aircraft Design and Optimization (PrADO) used here (Heinze, 1994), where modules from various engineering disciplines are consecutively iterated within a synthesis code until preselected design parameters reach convergence and feasible, physics-based solutions are identified. In that process, particularly to derive low-noise solutions, aerodynamics, engine performance and flight simulation can be considered in great detail, e.g., by replacing simulation modules based on simple methods by high-fidelity data. For example, for adequate engine noise predictions, the engine simulation within the conceptual design synthesis process can be replaced by high-fidelity simulation data.

The operating condition of the vehicle determines its noise emission and therefore the noise impact on the ground. To model approach and departure trajectories with underlying configurational settings such as engine operation or high-lift usage, the flight simulation code Flightpaths for Noise Analyses (FlipNA) (Blinstrub, Bertsch, & Heinze, 2018) was integrated into PrADO.

Noise calculation capabilities were introduced into PrADO with the software tool PANAM (Bertsch, 2013), to predict and assess aircraft noise and use it as a design objective within the conceptual design phase. Within this design phase, major aircraft design parameters, e.g., engine selection or wing area, are still subject to modifications, and thus can be adapted and optimized with respect to the overall noise performance. Noise assessment within this design stage can result in fundamental changes and modifications to the aircraft architecture if low-noise performance is the overall goal. Furthermore, approach and departure flight trajectories can be tailored to any vehicle to meet certain objectives such as noise. This simulation process has already been used to identify promising low-noise aircraft concepts along their individually optimized flight trajectories (Bertsch, Heinze, & Lummer, 2014).

### *2.3. Noise emission prediction*

For the subsequent auralization of aircraft flyovers, noise emission data along the aircraft trajectory is predicted. In that process, attention must be paid to the fact that auralization sets high requirements on temporal and frequency resolutions of the acoustic emission description, as well as on temporal smoothness of the emission data.

#### 2.3.1. *Major noise sources*

The noise emission of the major sources of the aircraft is calculated by the aircraft noise prediction tool PANAM (Bertsch, 2013). It requires high-fidelity engine data, a valid design synthesis and a flight procedure as input. PANAM contains parametric calculation models for various componential noise sources of an aircraft. It separately describes engine and airframe noise sources as a function of aircraft design geometries and operational conditions. For each (point) source, far-field sound pressure levels can be obtained for a large range of frequencies and radiation angles at a reference distance of 1 m to the point source. Also acoustic installation effects, for example engine integration on board of an aircraft, may be considered. Possible acoustic shielding is estimated by the code SHADOW (Lummer, 2008), which is a ray-tracing tool to evaluate engine noise shielding. It delivers spectral sound pressure level differences in dB from the vehicle's 3D geometry, e.g. for an installed engine as compared to the engine under free-field conditions.

For the auralization, data of different componential noise sources are summarized into three contributions: (1) airframe broadband, (2) engine broadband, and (3) engine fan tones. The emission data of the selected contributors are extracted per sound emission angle for defined receiver positions, i.e. accounting for source directivity. The selected emission data is

sampled in source time steps of half a second. It comprises one-third octave band spectra (20 Hz to 20 kHz) for the broadband contributions, and sound pressure levels at specific frequencies for the tonal contributions. Convective and Doppler amplification, but not Doppler frequency shift which is simulated in the propagation filtering (see Section 2.4.2), are included according to the radiation angle. The resulting emission data set, i.e., spectral data for each source contribution, time step and emission angle to the selected receiver position, is used as input to the auralization process, as described in (Pieren, Bertsch, Blinstrub, Schäffer, & Wunderli, 2018).

### 2.3.2. *Airframe cavity tones*

Relatively small structures at the airframe can lead to relevant narrowband aeroacoustic sound sources. Their acoustical behavior is difficult to predict and not included in the above aircraft noise prediction process to date. The probably best documented example of such narrowband sounds are the wing cavity tones from the aircraft of the Airbus A320 family (Dobrzynski W. , 2010; Zellmann, Jäger, & Schlatter, 2018). They originate from fuel overpressure ports (FOPP; see Figure 2.2) that are four distributed openings with a diameter of about 10 cm in the lower wing surfaces. To mitigate this noise source, a vortex generator may be installed (Dobrzynski W. , 2010). This device can be mounted in front of the opening as a retrofit measure (shown in Figure 2.2).

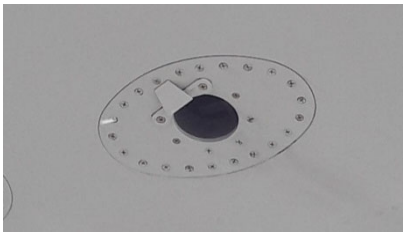

Figure 2.2: Photography of a fuel overpressure port (FOPP) of an Airbus A320 with an installed vortex generator (photography by the authors).

For the wing cavity tones of the A320 family (the reference case of the studied application; see Section 3) an emission model was developed in this study. The model is based on acoustical data from the sonAIR field measurement campaign (Zellmann, Schäffer, Wunderli, Isermann, & Paschereit, 2018; Wunderli, et al., 2018). It was found that in most cases two distinct peaks appear in the sound pressure spectra. The presence of two frequencies can be attributed to two specific geometries of the cavities behind the openings. This spectral pattern is perceived as a fluctuating double tone. For the de-Dopplerized data, the associated peak frequencies were found to be rather constant and located at 550 and 620 Hz, respectively. No indication for distinctive source directivity was found. However, the sound power of this source shows strong speed dependence. In the range of Mach 0.2 to 0.3, the sound power was found to be related to the $10^{th}$ power of the vehicle airspeed. For example, an airspeed increase from 80 to 100 m/s leads to a remarkable increase in sound power by 10 dB. Using the above measurement data, for both spectral components, the following approximation for their sound power level $L_W$ in dB as a function of the Mach number $M$ was derived within this work:

$$L_W = 125 + 120\,|\log_{10}(M)| - 200\,|\log_{10}(M)|^2, \text{for } M < 0.4 \tag{1}$$

### 2.3.3. *Transitions between configurations and operational conditions*

The described simulation process accounts for various flight phases that differ with respect to aircraft configuration and operational conditions. This source variability has to be considered in noise assessment. This is done here by simulating the impact at multiple spatially distributed, non-moving, ground-based receivers (Section 3.2.3). For a single flight, the receiver positions may be chosen such that no immediate source changes occur during the flyover event. With that, the aircraft state can be held fixed during each flyover event. This significantly simplifies the auralization process and corresponds to how aircraft auralizations are typically made to date.

However, when comparing the impact of different flight procedures it gets impossible to select representative receiver positions that spatially sample the flight trajectories without conflicting with changes in the aircraft state, e.g., deployment of the high-lift system along the trajectory. Thus, for such comparisons it becomes mandatory to consider the transitions between aircraft configurations and operational conditions. Flight trajectories are typically simulated segment-wise, and discontinuities in airspeed, thrust (and thus fan speed N1), or configuration may occur between segments. Such immediate changes do not cause issues in noise mapping where integral noise indicators are calculated over the flyover event. However, preliminary auralizations in the context of this study revealed that sudden changes in the source description can be audible. Abrupt changes in the sound were perceived as artefacts, and the simulation was therefore assessed as unnatural. Therefore, the source description over time was enhanced to increase plausibility of the simulation.

As an example, the fan speed N1 is required to behave smoothly because it directly steers the frequencies of the fan harmonics. This is accomplished by temporally smoothing the flight trajectory data before the emission level prediction. Other examples are changes in the configurational setting such as landing gears, flaps and slats. For these changes, realistic transition times are introduced. The extension of the landing gears is simulated by linearly increasing the gear length parameter from zero to the full length over a time span of five seconds. Transitions between flaps and slats settings are simulated by continuously changing their angles with maximum four degrees per second.

## 2.4. *Auralization of synthetic flyovers*

Using the technique of auralization, synthetic aircraft flyovers in a virtual environment at certain receiver positions near the ground are artificially made audible, including the creation of a spatial impression (i.e., sound source localization along arbitrary three-dimensional flight trajectories), as shown in Figure 2.3.

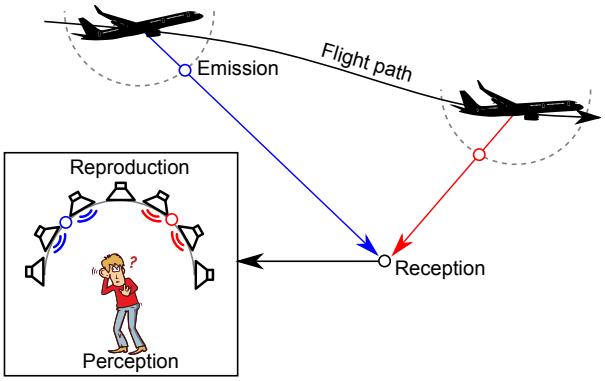


Figure 2.3: Concept of converting acoustic emission data along the flight path into a perceivable sound field at a virtual receiver position using a loudspeaker array in a laboratory setup.

The principle of auralization according to the definition by (Vorländer, 2008) is the separate representation of sound generation, propagation, and reproduction. As illustrated in Figure 2.4, the auralization process followed here is structured into the three modules emission synthesis, propagation filtering, and reproduction rendering. The audible sounds are thereby completely artificially created by digital sound synthesis techniques. The following sections describe the three involved processing steps.

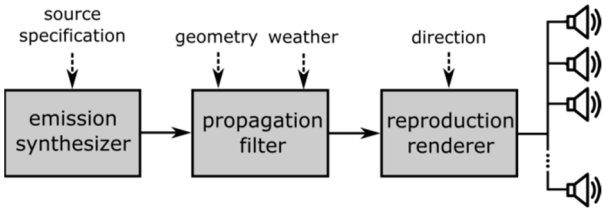


Figure 2.4: Signal flow chart of the auralization process to synthesize an environmental acoustical scene.

### 2.4.1. *Emission sound synthesis*

The underlying assumption for emission synthesis is that each componential noise source of the aircraft can be represented by an incoherent, concentrated point source with an individual frequency-dependent directivity. In the first processing step of Figure 2.4, sound signals for each componential source are generated. For this, the predicted noise emission data from Section 2.3 is used as input. The source signals are attributed to a reference distance to the aircraft and in the direction of the receiver. The resulting time signals are synthesized using parametric sound synthesis techniques, i.e. by algorithms that do not rely on audio recordings. Except for the new method for wing cavity tones, available state-of-the-art methods for environmental sound synthesis (Arntzen & Simons, Modeling and synthesis of aircraft flyover noise, 2014; Rizzi, Aumann, Lopes, & Burley, 2014; Pieren, Heutschi, Müller, Manyoky, & Eggenschwiler, 2014; Pieren, Bütler, & Heutschi, 2016) are used.

Separate source signals are generated for

- engine fan tones,
- engine broadband noise (jet + fan),
- airframe broadband noise and
- wing cavity tones.

The fan harmonics (engine fan tones) are generated using additive synthesis using a series of oscillators. Each numerically controlled oscillator is individually steered by a time-variant frequency and amplitude control function. The first five fan harmonics are individually synthesized. The other three source signals are generated by subtractive synthesis where white noise signals are processed by digital, time-variant filters. The spectral shaping of the broadband noise components is performed in 1/3 octave bands.

For the cavity tones, a specific synthesis model was developed within this study. Initial attempts were made using additive synthesis. However, listening comparisons to recordings revealed that this approach produces a very different hearing impression. Literature suggests that cavity tones are generated by a Helmholtz resonator that is excited by a grazing airflow (Meissner, 2002). This conception suggests that cavity tones have a random excitation pattern and a certain spectral bandwidth. This is the motivation for the developed model based on subtractive synthesis.

The total sound pressure signal of the cavity tones consists of the sum of $k$ individually generated cavity tones. The corresponding sound pressure signal as a function of the source time $t$ is formed by

$$p_{\mathrm{e,cav}}(t) = \sum_k A_k(t) \int_{-\infty}^{\infty} w_k(\tau) h_k(t-\tau) d\tau \tag{2}$$

with the amplitudes $A_k$, random white Gaussian noise signals $w_k$, and filter functions $h_k$ that are convolved with the noise signals. The time-varying amplitudes scale the signals to ensure the pre-defined sound pressure levels. For the wing cavity tones, the amplitudes are calculated using Equation (1) where the Mach number $M$ changes over time $t$ during flyover:

$$A_k(t) = p_0 10^{[L_W(M(t))-C]/20} \tag{3}$$

with the reference sound pressure $p_0 = 20$ µPa and the power-to-pressure conversion term $C = 10 \log_{10}(4\pi) \approx 11$ dB for an omnidirectional source and spherical propagation to one meter. The time signal $h_k$ is defined in the frequency domain by

$$H_k(s) = \mathcal{L}\{h_k\}(s) = \frac{\omega_{0,k}^2}{s^2 + 2\zeta_k \omega_{0,k} s + \omega_{0,k}^2} \cdot H_{\mathrm{BP},k}(s) \tag{4}$$

with the complex frequency variable $s$, the angular resonance frequency $\omega_{0,k} = 2\pi f_{\mathrm{cav},k}$, and the damping ratio $\zeta_k$. $H_{\mathrm{BP},k}$ is the frequency response of a bandpass filter with center frequency $f_{\mathrm{cav},k}$ and a (relative) bandwidth of one-third octave, i.e. $0.23 f_{\mathrm{cav},k}$. The bandwidth $B$ in Hz of the peak filter (i.e. the fraction in Equation (4)) is given by $B = 2\zeta_k f_{\mathrm{cav},k}$. On that basis, discrete-time infinite impulse response (IIR) peak filters are designed using a pre-warped bilinear transform:

$$s = \frac{\omega_{0,k}}{\tan\left(\frac{\omega_{0,k}}{2 f_s}\right)} \cdot \frac{z-1}{z+1} \tag{5}$$

with the audio sampling rate $f_s$ in Hz and the complex-valued digital frequency $z$. The convolution in Equation (2) is thus realized in discrete time by processing each noise signal $w_k$ with a specific peak filter and a specific bandpass filter in series.

The synthesis parameters of the wing cavity tones were set based on field measurements. The two peak frequencies, $f_{\mathrm{cav}}$, were set to 550 and 620 Hz, respectively, and the corresponding damping ratios were both set to 0.002, corresponding to bandwidths $B$ of about 2 Hz. Figure 2.5 compares measured sound pressure data of a flyover with a synthesized signal generated which the described model.

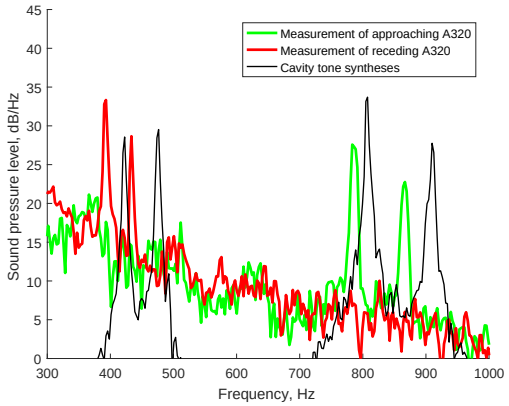


Figure 2.5: Narrowband sound pressure spectra with distinct wing cavity tones from a measured Airbus A320 at Mach 0.3 during approach. The Doppler effect shifts the two peaks from around 800 Hz (green) to 400 Hz (red) during the flyover event. Corresponding syntheses with the proposed model are shown in black. Analysis length is two seconds.

### 2.4.2. *Propagation filtering*

In the second processing step in Figure 2.4, the effects of sound propagating from the source to the receiver are simulated separately for each source contribution. In that process, a source (emission) sound pressure signal, $p_{\mathrm{e}}(t)$, is transformed into a receiver sound pressure signal, $p_{\mathrm{r}}(t')$. The model conception behind the simulation is that the most relevant propagation effects are independently described and modeled, similarly to current engineering propagation models. However, in auralization this is realized in the time domain by using filters. Because the propagation conditions change during the flyover, time-variant filters are utilized.

The considered propagation effects are

- Doppler frequency shift,
- geometrical spreading,
- air absorption,
- ground effect and
- turbulence effect.

Their simulation is realized by a network of time-variant digital filters as illustrated in Figure 2.6. The (arithmetic) sum over the contributions of all sub-sources at the receiver position corresponds to the received sound pressure signal which is stored as a monophonic digital audio signal.

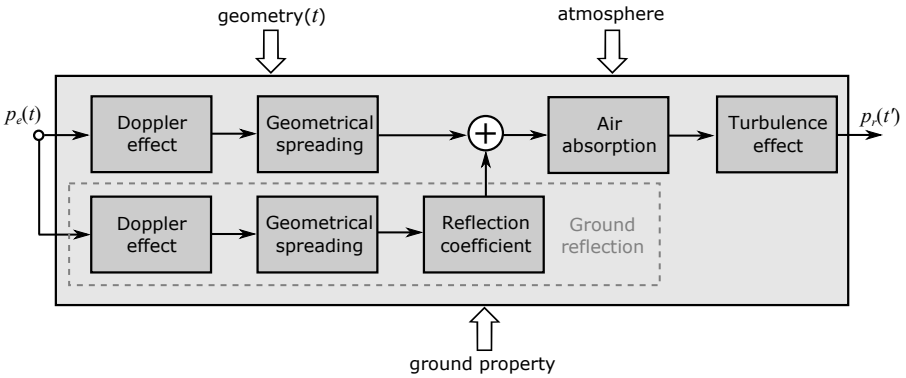


Figure 2.6: Propagation simulation in the time domain by a network of time-variant digital filters representing different wave propagation phenomena.

Geometrical spreading for the far-field of a point source is implemented by realizing the $1/d$ pressure dependence, where $d$ denotes the propagation distance. Doppler frequency shift is implicitly accounted for by modeling the time-variable propagation delay from source to receiver. It is realized by a fractional delay using bandlimited interpolation to keep audible artefacts (e.g. aliasing) low (Pieren, Bütler, & Heutschi, 2016). Ground effect is modeled by an additional signal path for ground reflected sound that interacts with the direct sound path. The interaction of the wave with the ground is simulated by introducing a filter representing the frequency-dependent reflection coefficient. For the latter a spherical wave reflection at an infinitely extended, locally reacting impedance plane is assumed. The ground impedance is predicted as a function of the airflow resistivity of the ground by the (Delany & Bazley, 1970) model.

Attenuation due to atmospheric absorption is modeled for an inhomogeneous atmosphere and for a near-ground receiver (height $\approx 0$). A stratified atmosphere is assumed that is described by the collection of height profiles, $\mathcal{M}(z)$, for air temperature, relative humidity and static pressure, where $z$ denotes altitude. The atmospheric attenuation, $A_{\mathrm{atm}}$, in dB as a function of the frequency $f$ is calculated accounting for the height-dependent properties of the atmosphere and propagation path length, i.e. source–receiver distance. For that, attenuation is integrated along the propagation path using the approximations

$$A_{\mathrm{atm}}(t) = \int_{\boldsymbol{r}_{\mathrm{receiver}}}^{\boldsymbol{r}_{\mathrm{source}}(t)} \frac{\alpha(\boldsymbol{r})}{1000} ds \cong \frac{d(t)}{1000}\bar{\alpha}(t) \cong \frac{d(t)}{1000}\frac{1}{N}\sum_{i=1}^{N} \alpha\left\{\mathcal{M}\left(\frac{iz_{\mathrm{S}}(t)}{N}\right)\right\} \tag{6}$$

where α is the local atmospheric absorption coefficient in dB/km for the frequency $f$ in Hz at location $\boldsymbol{r}$ calculated according to ISO 9613-1 (ISO, 1993), $d$ denotes the source–receiver distance in meter, $\bar{\alpha}$ is the effective (spatially averaged) absorption coefficient, $z_{\mathrm{S}}$ is the instantaneous source height above ground at the receiver position, and $N$ is the number of considered height segments for the discretization of the propagation path. In this work, $N$ was set to 20. From $A_{\mathrm{atm}}$ a finite impulse response (FIR) filter with 1024 taps is designed using the inverse fast Fourier transform (IFFT) (Pieren, Bütler, & Heutschi, 2016; Heutschi, et al., 2014)

Wave propagation through a turbulent atmosphere leads to phase and amplitude modulations. Particularly turbulence-induced amplitude modulations (AM) are commonly distinctly audible in aircraft noise and are therefore introduced to increase plausibility. The developed model considers the facts that turbulence-induced AM is of random nature and depends on frequency and the propagation distance. Literature suggests a magnitude dependency of $f^2d$ and a saturation effect (Daigle, Piercy, & Embleton, 1983). On that basis, turbulence-induced AM is modeled by a high shelf filter with distance-dependent transition frequency and a random, time-dependent gain (Heutschi, et al., 2014). In contrast to (Heutschi, et al., 2014), who used a linear phase FIR filter, here a minimum phase first-order IIR filter is suggested with the transfer function

$$\mathrm{H}_{\mathrm{turb}}^{t}(s) = \frac{\omega_c + g(t)s}{\omega_c + s} = \frac{\omega_c}{\omega_c + s} + \left(1 - \frac{\omega_c}{\omega_c + s}\right) g(t) \tag{7}$$

with the complex variable $s$, the high-frequency gain $g$, and the angular transition frequency

$$\omega_c = 2\pi \frac{9000}{\sqrt{d(t)}} \tag{8}$$

where $d$ is the source–receiver distance in meter. The formulation on the right hand side of Equation (7) reveals how the high shelf filter can be implemented with a first-order Butterworth low-pass filter. Equation (8) ensures the required frequency-distance behavior. The gain $g$ is set to $g(t) = 10^{G(t)/20}$, where the gain signal $G$ in dB is created with a random process and is normally distributed with mean value $\mu = -0.115\sigma^2$ and standard deviation $\sigma$. This setting ensures energy-neutrality of the simulated turbulence effect. Figure 2.7 displays magnitude frequency responses of the turbulence filter.

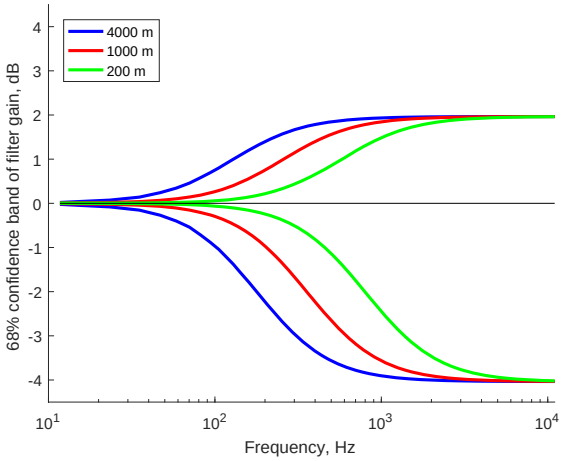


Figure 2.7. Statistical magnitude frequency responses of the developed turbulence filter for different propagation distances. The asymmetry along the 0 dB line assures energy-neutrality of the processing.

Reflections at and shielding from near-ground objects such as buildings are not considered. Also curved sound propagation paths or multiple ground reflections due to wind or temperature gradients are not modeled.

### 2.4.3. *Reproduction rendering and sound reproduction*

In the third step according to Figure 2.4, the resulting receiver sound pressure signal, $p_r(t')$, is fed to a multichannel audio reproduction system with the aim of simulating a listening experience of a moving sound source being above the head (cf. Figure 2.3). This allows the creation of a spatial impression of a flyover. For that, the corresponding time-variant angles of sound incidence at the receiver position are needed. Using this directional information, the monophonic signal is distributed to a 3D loudspeaker array to create a perceivable sound field. The reproduction rendering, i.e. the calculation of the speaker feeds, is realized by a dual-band amplitude panning technique (Taghipour, Pieren, & Schäffer, 2019). Furthermore, a crossover splits off the low frequency signal content for the subwoofers. Each channel of the reproduction system is calibrated using a sound level meter placed at the center of the listening zone.

### 2.4.4. *Listening test facility*

For the present study, the listening test facility AuraLab at the corresponding author's institution, Empa, was used. The facility has a separate listening room and a control room for audio-visual supervision. The listening room features high structure- and airborne sound insulation, low background noise (below 7 dBA) and controlled room acoustics with a reverberation time as low as $T_{mid} = 0.11$ s. At the time of the study, the laboratory contained a hemispherical loudspeaker array with 15 satellite speakers and two subwoofers. Figure 2.8 shows a photograph of the laboratory set-up. The satellite speakers of the type Neumann KH 120 A were arranged in pentagons on three levels with elevations 0°, 30° and 60° from the listening plane at a listening distance of 2 m. The two subwoofers of type Neumann KH 805 were positioned on the floor. The loudspeakers were connected to a 16-channel digital audio controller of the type Xilica Neutrino A0816 (sampling rate 48 kHz). Dante (Digital Audio Network Through Ethernet) was used to send the pre-rendered multi-channel digital audio streams from a computer in the control room to the audio controller. A touchscreen near the listening spot was connected to the same computer for remote control.

Figure 2.8. Laboratory set-up of the listening experiment in Empa's AuraLab with a hemispherical loudspeaker array, subwoofers and a display screen for the listening tests.

## *2.5. Perception-based evaluation*

Perception-based evaluation was performed by means of a laboratory listening experiment in the listening test facility AuraLab. The experimental design has to be specifically adapted to the endpoint of the evaluation. The present experiment

was designed for the evaluation endpoint short-term noise annoyance, as explained in detail in Section 3.3. Another endpoint, such as audibility of tonal components, would require another experimental design.

## 3. Application

### *3.1. Study overview*

This application study focuses on experimental short-term noise annoyance of flight approaches of civil tube-and-wing transport aircraft. The approach (in contrast to departure or cruise) was selected for this study due to its complexity with varying prominence of the different noise sources as perceived on the ground. Three aircraft types with two flight procedures each, making a total of six virtual approaches, are examined (cf. Figure 3.1). These test cases are built up around a reference case which corresponds to a known, existing reference aircraft ('Reference') along a standard landing procedure ('Standard'). On that basis, two different levels of vehicle technology evolutions with different time horizons are introduced, i.e., a variant with added low-noise airframe measures ('Retrofit') and a novel low-noise vehicle design ('Game changer'). Besides the Standard procedure also 'Tailored' flight procedures are investigated for each vehicle. The simulated cases are physically possible and considered as technically feasible. This set-up allows investigating the effects of different aircraft design levels and alternative flight procedures separately as well as in their combination.

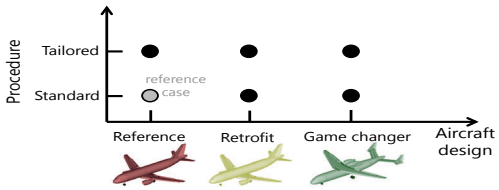


Figure 3.1. Overview of the test cases (circles) with three aircraft designs and two procedures resulting in six virtual approaches.

### *3.2. Investigation cases*

A perception-based evaluation presumes the definition of a receiver in the virtual environment. For representativeness, the six test cases are investigated at four virtual receiver positions. The experiment was scheduled with a full factorial design with respect to the variables aircraft type, flight procedure and receiver position, making a total of 24 (6 virtual approaches × 4 receiver positions) investigation cases.

#### 3.2.1. *Aircraft types*

The modeled aircraft are medium-range, narrow-body, commercial passenger twin-engine jet airliners with tube-and-wing architecture. The vehicles are designed to meet the identical TLAR. Table 1 gives an overview of the three modeled aircraft (Reference, Retrofit and Game changer).

Table 1. The three aircraft types of the experiment.

| | Aircraft type | | |
|---|---|---|---|
| | Reference | Retrofit | Game changer |
| Engine type | Conventional turbofan | Conventional turbofan | Conventional turbofan |
| Engine bypass ratio | 6 | 6 | 6 |
| Vehicle architecture | Conventional | Conventional | Engine noise shielding |
| Low-noise airframe | No | Yes | Yes |

As Reference aircraft, an existing type was selected that is relevant with respect to number of aircraft, movements and noise complaints. The Reference is a conventional aircraft, similar to an Airbus A319-100 with conventional turbofan engines. A design mission range of 3330 km, 124 passengers, a cruise Mach number of 0.76 define the selected TLAR. For this aircraft, high-fidelity engine data was taken from (Deidewig, 1998).

Promising low-noise airframe technologies for current vehicles were identified by (Pott-Pollenske, Wild, & Bertsch, 2014). These modifications are implemented in the Retrofit vehicle as retrofit measures to the reference aircraft. The selected low-noise airframe technologies and their noise reduction are:

- landing gear mesh fairing (Dobrzynski, et al., 2006; Dobrzynski, et al., 2009): landing gear noise −3 dB,
- porous side edges (Herr, 2007; Delfs, 2006): flap noise −5 dB,
- slat droop nose design (Bold & Pagnitz, 2012; Pott-Pollenske, Wild, & Bertsch, 2014): slat noise −6 dB.
- FOPP vortex generators (Dobrzynski W. , 2010): avoidance of wing cavity tones.

The underlying assumption for this application example is that the installation of the modifications does not change aerodynamics or mass.

Based on the Reference, a large low-noise design study had been previously performed (Bertsch, 2013). Basic geometrical design parameters were studied for their effect on noise on the ground of the overall aircraft, for instance the engine installation location, the vehicle architecture and the area and aspect ratio of wing and empennage. While the engine type was held constant in the aircraft design variations, the aircraft architecture was optimized for low-noise performance. In the 2013 study, additional low-noise technology was neither assumed for the engine noise sources nor for the airframe noise sources. The most promising low-noise aircraft variant (in earlier work denoted as "V-2") was included in this study as the Game changer. Due to its architecture (see Figure 3.2), it is subject to strong shielding of the fan noise. Further, jet-flap and gear-flap interaction noise is avoided, and the length of the landing gear is reduced. In addition, the aforementioned low-noise airframe technologies were installed in the Game changer, as indicated in Table 1.

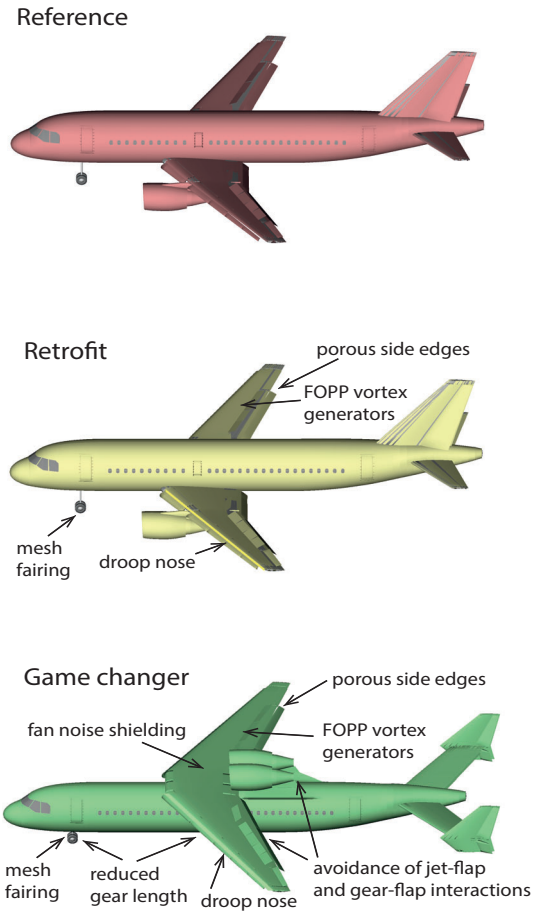


Figure 3.2: Visualizations of the studied aircraft designs with indicated low-noise modifications.

### 3.2.2. *Flight procedures*

All three vehicles are simulated along two different flight trajectories. Mainly the altitude, airspeed, and high-lift deployment are modified, as illustrated in Figure 3.3. All simulated landing procedures have the same flight track over ground and end on a fixed touch-down point on the runway. All flights are simulated to keep the required engine thrust to a minimum along the entire approach (close to engine flight idle).

First, all three aircraft are forced to perform the Standard (reference) procedure. This is similar to current standard landing procedures at major airports. The Standard procedure is predefined by the height profile, the airspeed profile and the setting of flaps, slats and landing gears as a function of the distance from the touch-down point. The Standard procedure has a glide angle of 3° during final approach.

Second, specific procedures were tailored for the three vehicles. Design objective for identification of these Tailored procedures was minimizing the spatially averaged Effective Perceived Noise Level (EPNL) on the ground below the simulated flight. The EPNL was chosen since it is the relevant metric for noise certification and tonal contributions are specifically considered. Variation of speed, altitude, and configurational setting yielded Tailored procedures with minimum mean EPNL. The Tailored procedures are limited to a maximum allowed glide angle of 4.49°, as indicated in Figure 3.3. Due to the assumption that the low-noise airframe measures will not affect flight performance, the Tailored procedures of both the Reference and the Retrofit vehicle are nearly identical. In contrast, the Tailored flight of the Game changer shows clear differences to the Tailored flight of the other two vehicles. The different architecture of the Game changer directly impacts aerodynamics, weights, and hence the flight performance (see airspeed profiles and corresponding high-lift deployments in Figure 3.3).

The Standard and Tailored procedures strongly differ (Figure 3.3). Extracting the high-lift system along the approach increases the EPNL for all three vehicles due to prevailing airframe noise dominance, even if low-noise measures are applied. Consequently, an optimization toward low-noise flight trajectories will avoid early high-lift deployment.

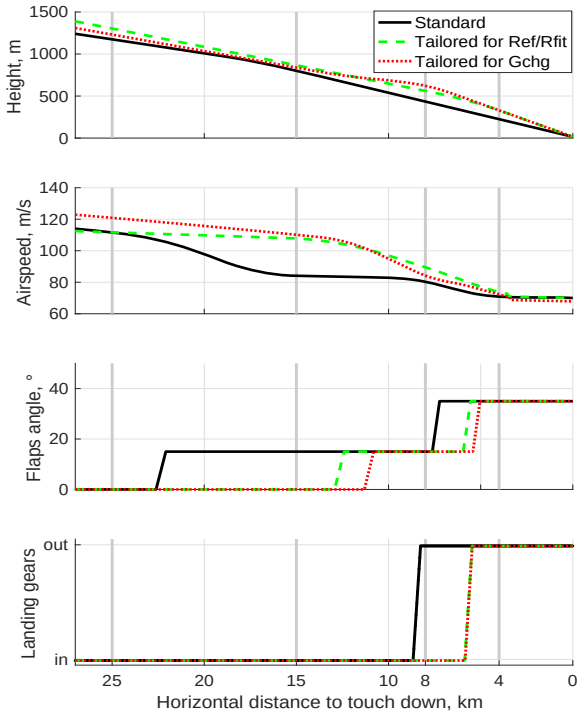


Figure 3.3. The simulated flight procedures in terms of aircraft altitude, airspeed, flaps angle, and position of landing gears. The Standard procedure and the Tailored procedures for the Reference (Ref), Retrofit (Rfit) and Game changer (GChg) vehicle are shown. The four receiver positions are indicated by bold vertical gray lines.

### 3.2.3. *Receivers*

For the study, four receiver positions were selected at distances of 4 to 25 km to the touch-down point (cf. Figure 3.3). The positions were chosen for (i) representativeness, since residents around airports are located in various distances, and (ii) to capture different flight phases from clean configuration to all-set. The resulting trajectory parameters in close proximity to the selected receiver positions are given in Table 2.

Table 2. Trajectory parameters in close proximity to the selected receiver positions.

| | | Aircraft | All | Reference/Retrofit | Game changer |
|---|---|---|---|---|---|
| | | Procedure | Standard | Tailored | Tailored |
| Receiver position | 4 km | Height, m | 224 | 329 | 331 |
| | | Speed, m/s | 71 | 74 | 72 |
| | | Flaps angle, ° | 35 (+gears) | 35 (+gears) | 35 (+gears) |
| | 8 km | Height, m | 434 | 561 | 622 |
| | | Speed, m/s | 80 | 89 | 84 |
| | | Flaps angle, ° | 15 (+gears) | 15 | 15 |
| | 15 km | Height, m | 801 | 867 | 838 |
| | | Speed, m/s | 84 | 108 | 110 |
| | | Flaps angle, ° | 15 | 0 | 0 |
| | 25 km | Height, m | 1174 | 1303 | 1231 |
| | | Speed, m/s | 112 | 112 | 121 |
| | | Flaps angle, ° | 0 | 0 | 0 |

Receiver heights were chosen as 1.2 m above ground, which is a common height for environmental noise measurements and the standard height of the ears of a seated person. The receiver orientations were chosen as facing 90° to the flight direction.

#### 3.2.4. *Receiver environment and atmospheric conditions*

For the ground effect simulation, a flat grassy terrain was assumed with an airflow resistivity of 200 kPa s/m$^2$. For air absorption simulation, the ICAO standard atmosphere with respect to static pressure and temperature (ICAO, International Civil Aviation Organization, 1993) and a constant relative humidity of 70% were taken. The speed of sound was set constant to 344 m/s. No wind was assumed and the degree of turbulence was held constant.

### *3.3. Perception-based evaluation*

#### 3.3.1. *Stimuli*

For the 24 investigation cases (see Section 3.2), the flight direction was varied (right to left or vice versa), which resulted in a total of 48 stimuli for the experiment (3 aircraft types × 2 flight procedures × 4 receiver positions × 2 flight directions). Stimuli duration was set to 30 s each, centered on the time when the aircraft is directly overhead. For the experiment, the stimuli set was subdivided into two subsets of 24 stimuli with fixed flight direction.

The audio signal processing to create the acoustical stimuli was performed with the synthesis methods described in Section 2.4. The corresponding audio files for playback were pre-rendered digitally with an audio sampling rate $f_s$ of 48 kHz.

#### 3.3.2. *Experimental procedure*

The listening experiment aimed at assessing short-term noise annoyance reactions to different aircraft technologies. The experiment was approved by the ethical committee of the first author's institution, Empa. It followed general guidelines such as (Nordtest, 2002) or (Ellermeier, Hellbrück, Kohlrausch, & Zeitler, 2008), and was conducted similarly to (Schäffer, et al., 2016). The acoustical stimuli were presented as treatments in a within-subject design, i.e., all subjects were exposed to all investigation cases. The subjects participated individually, one subject at a time, doing focused tests where they deliberately listened to and rated the stimuli regarding annoyance. The subjects used the ICBEN 11-point scale (Fields, et al., 2001), where 0 represents the lowest and 10 the highest annoyance rating, to answer the following question during or after playback of each stimulus (taken from (Schäffer, et al., 2016)) (in German): "When you imagine that this is the sound situation in your garden, what number from 0 to 10 best shows how much you would be bothered, disturbed or annoyed by it?"

In short, the experimental procedure consisted of (1) a short introduction to the research topic, (2) filling out a consent form for study participation, (3) a questionnaire about self-reported hearing capability and well-being as inclusion/exclusion criteria for study participation, (4) the actual listening experiment with an orientation (example stimuli), exercise ratings and the main experiment, and (5) a post-experimental questionnaire with questions on subjects' characteristics. A software application with a graphical user interface guided the subjects throughout the experiment, with automatic playback of the stimuli and recording of the entered annoyance ratings. The experiment took about 45 min per subject.

For the experiments, the subjects were randomly assigned to one of the subsets of 24 stimuli with fixed flight direction (see above) in a randomized-block design (Cohen, 2013). Within these subsets, a partially counterbalanced design (Latin square blocks) was chosen for the presentation order of the receiver position, while the six stimuli per position (3 aircraft types × 2 flight procedures) were randomized.

#### 3.3.3. *Human subjects*

Thirty-two subjects (10 females, 22 males) with self-reported normal hearing participated in the study. They were 22 to 63 years old (mean of 38.4 years).

#### 3.3.4. *Statistical analysis*

In a first step, the annoyance ratings were exploratively analyzed and visualized (e.g., mean values of the investigation cases). Thereafter, the ratings were analyzed by means of linear mixed-effects models that allow separating fixed effects (here, in particular the investigation cases) and random effects (the subjects, randomly chosen from a population). Such multilevel analysis (here, with the lower level being the individual ratings and the upper level being the subjects) has previously proven useful in transportation noise annoyance studies, e.g. (Groothuis-Oudshoorn & Miedema, 2006; Trolle, Marquis-Favre, & Klein, 2014; Gille, Marquis-Favre, & Weber, 2016; Wilson, Pettit, Wayant, Nykaza, & Armstrong, 2017).

As fixed effects, the investigation cases were a priori tested. As the Tailored procedure is specifically designed for a certain aircraft type, the variables aircraft type and flight procedure were analyzed as one combined categorical variable ("AC_Proc", with 6 levels = combinations of 3 aircraft types × 2 flight procedures). The receiver position was accounted for as a continuous variable with the logarithm of the distance to touch-down. Further, the interaction between these two primary variables was tested to check whether annoyance to aircraft types and/or procedures changed with receiver position. Besides, also the flight direction as a categorical variable, the playback number of the stimuli to study possible simple order effects (Cohen, 2013), as well as the first presented receiver position to study primacy effects were tested. As described in more detail by (Schäffer, et al., 2016), several models of different degrees of complexity were tested to choose the final model. Model assumptions were checked and confirmed by means of residual plots. The goodness-of-fit of the final model was assessed according to (Nakagawa & Schielzeth, 2013) and (Johnson, 2014), using the marginal ($R^2_m$) and conditional

coefficients of determination ($R^2_c$) to quantify the variance explained by the fixed factors and by the fixed plus random factors, respectively.

## 4. Results and discussion

### *4.1. Verification of the synthetic flyovers*

#### 4.1.1. *Spectrograms*

The synthesized sound pressure signals at the virtual receiver positions can be interpreted as virtual measurement microphone signals, sometimes denoted as pseudo-recordings. This allows computing common noise indicators such as sound exposure levels (SEL) or maximum levels (Lmax). In addition, and in contrast to classical noise prediction, also psychoacoustic parameters such as loudness, sharpness and tonality, as well as time-frequency representations can be calculated. Spectrograms, i.e. visual time-frequency representations, can be used to illustrate and verify the effects of the simulated physical phenomena on sound pressure.

Spectrograms of four investigation cases of this study are exemplarily depicted in Figure 4.1. Besides the broad frequency content, they illustrate distinct temporal and spectral features of the synthetic flyover sounds. Discrete tonal components with decreasing frequencies over time due to the Doppler frequency shift are observed. Due to geometrical divergence, the highest levels occur around the flyover time (relative time 0 s in the graphs). High frequencies (above 2 kHz) are only received around this instant, because atmospheric absorption strongly attenuates the high frequency content with increasing propagation distance. The ground effect patterns ("u-shapes") signify that elevated receivers and phase-sensitive interaction of direct and ground reflected sound was simulated. The broadband temporal fluctuations with modulation frequencies in the order of seconds are due to the simulated atmospheric turbulence effect. The spectrograms show that this effect mainly influences mid and high frequencies and gets stronger at larger distances.

In Figure 4.1, various differences between aircraft and receiver positions are observed. For the Reference aircraft (left column), two tonal components around 500 Hz are due to the wing cavity tones, whereas the two components above 1 kHz are the first and second fan harmonic, respectively. The cavity tones are much more prominent at 15 km than at 4 km to touch-down which is due to their higher emission levels (because of the higher flight speed) and less spectral masking from other sources. In contrast, almost no tonal components are seen for the Game changer, which also exhibits lower sound pressure levels at the same receiver positions compared to the Reference. Differences in the ground effect patterns are due to the varying flight trajectories. The same applies to general differences in the turbulence effects, whereas subtle differences are due to their underlying random nature.

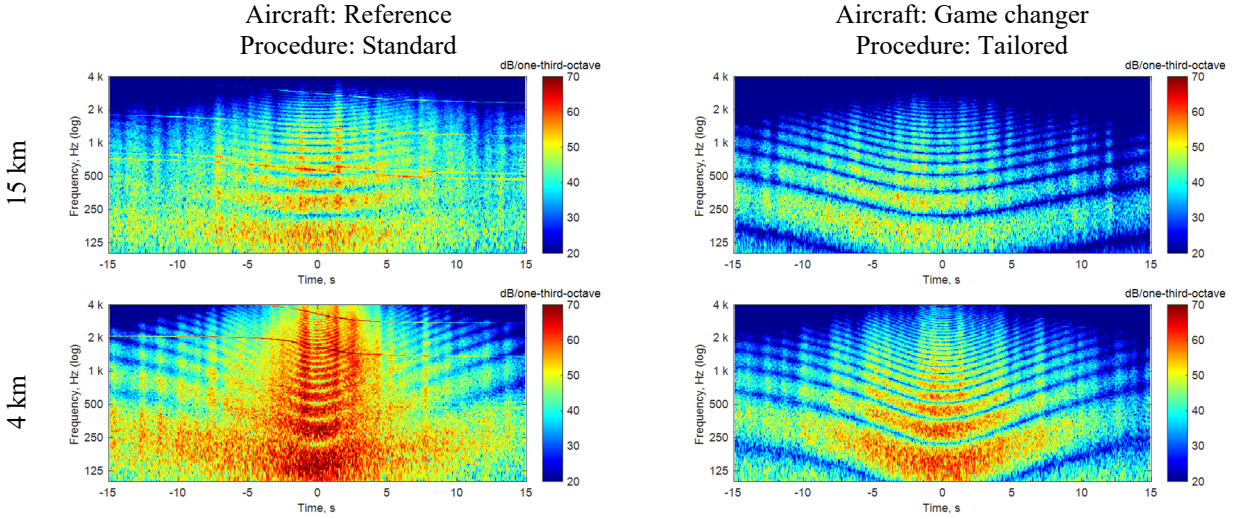


Figure 4.1. Spectrograms of synthesized sound pressure signals from simulated flyovers for the Reference aircraft on the Standard procedure (left) and the Game changer aircraft on its Tailored procedure (right), both for receiver positions 4 km (bottom) and 15 km (top) before touch-down, respectively.

#### 4.1.2. *Sound quality and plausibility*

The created sound signals do not contain any audible artefacts (e.g. zipper noise, clicks, distortion) and are of high sound quality. During spatial sound reproduction in the laboratory setup, continuous virtual source trajectories are perceived without any undesirable swelling or fading of the sounds during the flyovers.

An additional and more recent quality criterion for audio in virtual and augmented reality applications is toward plausibility (Rumsey, 2018). Plausibility is assessed by a subjective comparison to an inner reference and describes the perceived agreement of the listener's expectations with acoustic reality (Lindau & Weinzierl, 2012). No suspicious comments or remarks about plausibility were given by any of the subjects during or after the experiment, even though most of them had personal experience with aircraft noise and they were not aware that all the stimuli were fully synthetically generated. Highest expectations are expected from experts, making them candidates for possibly the most rigorous assessment. Here, acousticians and aircraft noise experts rated the stimuli as "very plausible".

### 4.2. Perception-based evaluation of aircraft technologies

The listening experiment revealed that, overall (i.e. arithmetic mean over all receiver positions), the aircraft types and flight procedures were both strongly linked to annoyance (Figure 4.2). This observation was confirmed by the mixed-effects model analysis (variable "AC_Proc", $p < 0.001$). Annoyance decreased in the order Reference > Retrofit > Game changer with respect to aircraft type, and in the order Standard > Tailored with respect to procedure. This means that both, the optimizations of aircraft types and procedures were successful regarding (reduced) annoyance. Most of the combinations of aircraft types and procedures are linked to significantly different mean annoyance values (Figure 4.2). Further, the efficiency of the Tailored procedure to reduce annoyance depends on the aircraft type. The largest benefit is obtained for the Retrofit. For this vehicle, engine noise has the largest relative contribution whereas for the Reference (no low-noise airframe measures) and the Game changer (shielded engines) the airframe rather than the engines is the dominant sound source along these approaches.

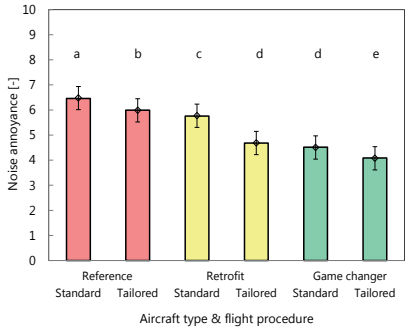


Figure 4.2. Mean noise annoyance of the six test cases. The bars show the measurements. The modelled data is shown by a diamond and the confidence interval. Statistically significant differences are indicated by differing letters above.

However, the above general observations do not (necessarily) represent a specific receiver position. First, annoyance significantly decreased with increasing distance of the receiver position to touch-down ($p < 0.001$). Further, there was a significant interaction between the variable "AC_Proc" and receiver position ($p < 0.001$). This indicates that the association of annoyance with aircraft type and flight procedure depends on the receiver position (Figure 4.3). In fact, the order of decreasing annoyance with aircraft type and procedure was similar for the positions at 4 and 8 km to touch-down, but quite different at the more distant positions. There, the Tailored flight procedure in most case was either not beneficial or even detrimental for annoyance. This is further visualized in Figure 4.4, which shows the annoyance ranking of the aircraft types and procedures as a function of the distance to touch-down. While the Reference is generally more annoying than the Retrofit and the Game changer, the ranking substantially changes with distance. Thus, optimization of aircraft design and procedure for a single receiver position is not sufficient, and inter- or extrapolation of results of a single or only a few positions to other situations is hardly possible. Further, optimization should be done airport-specific, particularly considering densely populated residential areas. Finally, the representativeness of the vehicle noise certification point for landings, which is even closer to the airport (2 km (ICAO, International Civil Aviation Organization, 2008)) than the situations studied here, where usually no/very few residents live, is questionable.

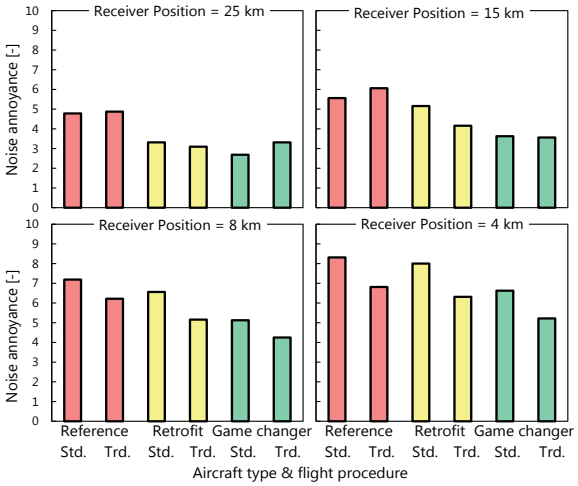


Figure 4.3. Mean noise annoyance of the investigation cases (Procedures: Std.=Standard, Trd.=Tailored). Observed data is shown for the six test cases at the four receiver positions separately.

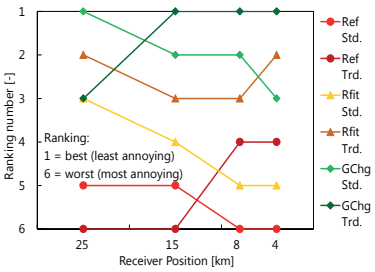


Figure 4.4. Ranking of the six test cases as a function of the receiver position, with respect to minimized annoyance (ranking: 1 = best [least annoying], 6 = worst [most annoying]) for the aircraft types (Ref=Reference, Rfit=Retrofit, GChg=Game changer) and procedures (Std.=Standard, Trd.=Tailored).

Besides the effects of the investigation cases, the mixed-effects model also confirmed that annoyance increased with increasing playback number ($p < 0.001$), which corroborates findings of (Schäffer, et al., 2016). Further, the first presented receiver position significantly affected the subsequent annoyance ratings of other positions ($p = 0.029$). The annoyance ratings increased with distance of the first presented position to touch-down, i.e. the larger the first distance the higher the annoyance ratings. Flight direction, in contrast, did not affect annoyance ($p > 0.66$).

Overall, the mixed-effects model established here represents the experimental observations well, explaining 86% of the variance ($R^2_m = 0.55$, $R^2_c = 0.86$).

## 5. Conclusions

Nowadays, noise assessment and communication of noise are accomplished using conventional noise indicators that consider neither the perception of sound, nor its health effects. To overcome these limitations, this article presents a comprehensive, multidisciplinary methodological approach that involves creating listening experiences of synthetic flyovers. In this study, the feasibility of perception-based evaluation of different future low-noise aircraft technologies was demonstrated. To do so, outputs from aircraft design and flight simulation were combined with auralization, the auralization model was substantially enhanced to adequately describe various aircraft specific phenomena, and the simulation chain was validated by expert ratings as well as in full listening experiments. The work goes beyond state-of-the-art in general, by using a multi-disciplinary approach to tackle the aircraft noise problem, as well as in specific technical aspects, e.g. by combining aircraft design with auralization.

The case study revealed that it is essential to model different sound sources of an aircraft, configurational transitions, as well as various sound propagation effects. Further, the listening experiments showed that (i) vehicle retrofitting and even more novel aircraft designs are beneficial for (reduced) noise annoyance, (ii) tailored flight procedures are less annoying than standard procedures, and (iii) maximum benefit may be obtained in combined optimization of aircraft design and flight procedures. Further, it was found that ranking of aircraft technologies with respect to noise annoyance critically depends on the receiver location, so that a single receiver (or certification) location is not sufficient for reliable assessment and thus for optimizations.

Finally, with the proposed approach the feasibility of perception-based evaluation of future low-noise aircraft technologies could be affirmed. This supports the movement for perception-influenced design in order to reduce the negative environmental impacts and adverse health effects caused by increased (air) traffic noise.

## Acknowledgements

The authors are most grateful to the subjects participating in the listening experiments. The work of Empa was partly funded by the Swiss Federal Office for the Environment (FOEN). The DLR activity was supported via a travel budget by the Projektförderung zur Internationalen Zusammenarbeit (PiZ). Some of the joint work was performed in the context of the research project Aircraft noise Reduction Technologies and related Environmental iMpact (ARTEM), which has received funding from the European Union's Horizon 2020 research and innovation programme under grant agreement No. 769350.

## References

Arntzen, M., & Simons, D. (2014). Modeling and synthesis of aircraft flyover noise. *Applied Acoustics, 84*, pp. 99-106.

Arntzen, M., Bertsch, L., & Simons, D. (2015). Auralization of novel aircraft configurations. *Proceedings of the 5th CEAS air and space conference, CEAS 2015* (pp. 1-11). Delft, Netherlands: The Institute of Acoustics.

Bartels, S., Márki, F., & Müller, U. (2015). The influence of acoustical and non-acoustical factors on short-term annoyance due to aircraft noise in the field — The COSMA study. *Science of the Total Environment, 538*, pp. 834–843.

Basner, M., Babisch, W., Davis, A., Brink, M., Clark, C., Janssen, S., & Stansfeld, S. (2014). Auditory and non-auditory effects of noise on health. *The Lancet, 383*, pp. 1325-32.

Bertsch, L. (2013). Noise Prediction within Conceptual Aircraft Design. *DLR Forschungsbericht, ISRN DLRFB-2013-20*. Germany: German Aerospace Center (DLR).

Bertsch, L., Heinze, W., & Lummer, M. (2014). Application of an Aircraft Design-To-Noise Simulation Process. *14th AIAA Aviation Technology, Integration, and Operations Conference, AIAA AVIATION Forum, (AIAA 2014-2169).* Atlanta: American Institute of Aeronautics and Astronautics, DOI: 10.2514/6.2014-2169.

Blinstrub, J., Bertsch, L., & Heinze, L. (2018). Assessment of the Noise Immission along Approach and Departure Flightpaths for Different SFB880 Vehicle Concepts. *2018 AIAA/CEAS Aeroacoustics Conference.* Atlanta: American Institute of Aeronautics and Astronautics, DOI: 10.2514/6.2018-2818.

Bold, J., & Pagnitz, M. (2012). *Design of a Silent Leading Edge (SLED).* Braunschweig, Germany: Report, Institut für Faserverbundleichtbau und Adaptronik.

Cohen, B. H. (2013). *Explaining psychological statistics.* Hoboken, NJ: John Wiley and Sons, Inc.

Daigle, G., Piercy, J., & Embleton, T. (1983). Line-of-sight propagation through atmospheric turbulence near the ground. *Journal of the Acoustical Society of America, 74(5)*, 1505.

Deidewig, F. (1998). *Ermittlung der Schadstoffemissionen im Unter- und Ueberschallflug.* Collogne, Germany: German Aerospace Center, DLR Forschungsbericht 98-10.

Delany, M. E., & Bazley, E. N. (1970). Acoustical properties of fibrous absorbent materials. *Applied Acoustics 3*, 105-116.

Delfs, J. (2006). *Anordnung eines Aerodynamisches Bauteils mit einer geschlitzten Hinter- oder Seitenkante in einer Stroemung.* Deutsches Patent- und Markenamt 2010: Deutsches Patent DE 10 2006 049616, 21.10.2006.

Dobrzynski, W. (2010). Almost 40 Years of Airframe Noise Research: What did we achieve? *Journal of Aircraft, 47(2)*, pp. 353-367.

Dobrzynski, W. M., Schöning, B., Chow, L., Wood, C., Smith, M., & Seror, C. (2006). Design and Testing of Low Noise Landing Gears. *International Journal of Aeroacoustics, 5(3)*, pp. 233-262.

Dobrzynski, W., Chow, L., Smith, M., Boillot, A., Dereure, O., & Molin, N. (2009). Experimental Assessment of Low Noise Landing Gear Component Design. *15th AIAA/CEAS Aeroacoustics Conference (30th AIAA Aeroacoustics Conference)* (pp. paper no. 2009-3276). Miami, Florida: AIAA.

Ellermeier, W., Hellbrück, J., Kohlrausch, A., & Zeitler, A. (2008). *Kompendium zur Durchführung von Hörversuchen in Wissenschaft und industrieller Praxis.* Berlin, Germany: Deutsche Gesellschaft für Akustik e.V.

Fields, J., De Jong, R., Gjestland, T., Flindell, I., Job, R., Kurra, S., . . . Schumer, R. (2001). Standardized general-purpose noise reaction questions for community noise surveys: research and a recommendation. *Journal of Sound and Vibration 242(4)*, 641-679.

Gasco, L., Asensio, C., & de Arcas, G. (2017). Communicating airport noise emission data to the general public. *Science of the Total Environment, 586*, pp. 836–848.

Gille, L.-A., Marquis-Favre, C., & Weber, R. (2016). Aircraft noise annoyance modeling: consideration of noise sensitivity and of different annoying acoustical characteristics. *Applied Acoustics, 115*, pp. 139–49.

Groothuis-Oudshoorn, C., & Miedema, H. (2006). Multilevel grouped regression for analyzing self-reported health in relation to environmental factors: The model and its application. *Biometrical Journal, 48(1)*, pp. 67-82.

Guski, R., Schreckenberg, D., & Schuemer, R. (2017). WHO Environmental Noise Guidelines for the European Region: A Systematic Review on Environmental Noise and Annoyance. *International Journal of Environmental Research and Public Health, 14(2)*, pp. 1539, 1-14.

Heinze, W. (1994). *Ein Beitrag zur quantitativen Analyse der technischen und wirtschaftlichen Auslegungsgrenzen verschiedener Flugzeugkonzepte für den Transport großer Nutzlasten.* Technical University Braunschweig: ZLR-Forschungsbericht 94-01, ISBN 3-928628-14-3.

Herr, M. (2007). Design Criteria for Low-Noise Trailing Edges. *13th AIAA/CEAS Aeroacoustics Conference (28th AIAA Aeroacoustics Conference)* (pp. paper no. 2007-3470). Rome, Italy: AIAA.

Heutschi, K., Pieren, R., Müller, M., Manyoky, M., Wissen Hayek, U., & Eggenschwiler, K. (2014). Auralization of Wind Turbine Noise: Propagation Filtering and Vegetation Noise Synthesis. *Acta Acustica united with Acustica, 100*, pp. 13-24.

ICAO, International Civil Aviation Organization. (1993). *Manual of the standard ICAO standard atmosphere, Doc 7488/3.* Montreal.

ICAO, International Civil Aviation Organization. (2008). *Annex 16 to the Convention on International Civil Aviation - Environmental Protection, Volume I - Aircraft Noise.*

ICAO, International Civil Aviation Organization. (2008). *Guidance on the Balanced Approach to Aircraft Noise Management, Doc. 9829, 2nd edition.*

ISO. (1993). ISO 9613-1. *Acoustics — Attenuation of sound during propagation outdoors — Part 1: Calculation of the absorption of sound by the atmosphere*. ISO.

Jagla, J., Maillard, J., & Martin, N. (2012). Sample-based engine noise synthesis using an enhanced pitch-synchronous overlap-and-add method. *Journal of the Acoustical Society of America, 132 (5)*, pp. 3098–3108.

Johnson, P. C. (2014). Extension of Nakagawa & Schielzeth's R2 GLMM to random slopes models. *Methods in Ecology and Evolution 5(9)*, S. 944-946.

Kephalopoulos, S., Paviotti, M., Anfosso-Lédée, F., & Van Maercke, D. (2014). Advances in the development of common noise assessment methods in Europe: The CNOSSOS-EU framework for strategic environmental noise mapping. *Science of the Total Environment, 482-483*, pp. 400–410.

Lindau, A., & Weinzierl, S. (2012). Assessing the Plausibility of Virtual Acoustic Environments. *Acta Acustica united with Acustica, 98*, pp. 804 – 810.

Lopes, L. V., & Burley, C. L. (2011). Design of the next generation aircraft noise prediction program: ANOPP2. *17th AIAA/CEAS Aeroacoustics Conference, AIAA*, (pp. 2011-2854). Oregon.

Lummer, M. (2008). Maggi-Rubinowicz Diffraction Correction for Ray-Tracing Calculations of Engine Noise Shielding. *14th AIAA/CEAS Aeroacoustics Conference.*

Meissner, M. (2002). Excitation of Helmholtz resonator by grazing air flow. *Journal of Sound and Vibration*, 382-388.

Nakagawa, S., & Schielzeth, H. (2013). A general and simple method for obtaining R2 from generalized linear mixed-effects models. *Methods in Ecology and Evolution 4(2)*, S. 133-142.

Nordtest. (2002). NT ACOU 111. *Acoustics: Human sound perception – Guidelines for listening tests (NT ACOU 111)*. Espoo, Finland: Nordtest.

Pieren, R., Bertsch, L., Blinstrub, J., Schäffer, B., & Wunderli, J. (2018). Simulation process for perception-based noise optimization of conventional and novel aircraft concepts. *AIAA Science and Technology Forum and Exposition.* Florida: DOI: 10.2514/6.2018-0264.

Pieren, R., Bütler, T., & Heutschi, K. (2016). Auralization of Accelerating Passenger Cars Using Spectral Modeling Synthesis. *Applied Sciences, 6, 5*, pp. 1-27.

Pieren, R., Heutschi, K., Müller, M., Manyoky, M., & Eggenschwiler, K. (2014). Auralization of Wind Turbine Noise: Emission Synthesis. *Acta Acustica united with Acustica, 100*, pp. 25-33.

Pieren, R., Heutschi, K., Wunderli, J., Snellen, M., & Simons, D. (2017). Auralization of railway noise: Emission synthesis of rolling and impact. *Applied Acoustics, 127*, pp. 34-45.

Pott-Pollenske, M., Wild, J., & Bertsch, L. (2014). Aerodynamic and Acoustic Design of Silent Leading Edge Devices. *20th AIAA Aeroacoustics Conference.* Atlanta: American Institute of Aeronautics and Astronautics, DOI: 10.2514/6.2014-2076.

Rizzi, S. (2016). Toward reduced aircraft community noise impact via a perception-influenced design approach. *45th International Congress and Exposition of Noise Control Engineering (InterNoise 2016).* Hamburg, Germany.

Rizzi, S., & Christian, A. (2016). A Psychoacoustic Evaluation of Noise Signatures from Advanced Civil Transport Aircraft. *22nd AIAA/CEAS Aeroacoustics Conference (AIAA 2016-2907)* (p. 16 pp.). Lyon, France: AIAA.

Rizzi, S., Aumann, A., Lopes, L., & Burley, C. (2014). Auralization of Hybrid Wing-Body Aircraft Flyover Noise from System Noise Predictions. *Journal of Aircraft, 51 (6)*, S. 1914-1926.

Rumsey, F. (2018). Evaluating AVAR - Goodby quality, hello plausibility? *Journal of the Audio Engineering Society, 66(12)*, pp. 1126-1130.

Sahai, A., Wefers, F., Pick, S., Stumpf, E., Vorländer, M., & Kuhlen, T. (2016). Interactive simulation of aircraft noise in aural and visual virtual environments. *Applied Acoustics, 101*, pp. 24-38.

Schäffer, B., Schlittmeier, S. J., Pieren, R., Heutschi, K., Brink, M., Graf, R., & Hellbrück, J. (2016). Short-term annoyance reactions to stationary and time-varying wind turbine and road traffic noise: A laboratory study. *Journal of the Acoustical Society of America, 139(5)*, pp. 2949–2963.

Taghipour, A., Pieren, R., & Schäffer, B. (2019). Short-term annoyance reactions to civil helicopter and propeller-driven aircraft noise: A laboratory experiment. *Journal of the Acoustical Society of America, 145(2)*, pp. 956–967.

Trolle, A., Marquis-Favre, C., & Klein, A. (2014). Short-term annoyance due to tramway noise: determination of an acoustical indicator of annoyance via multilevel regression analysis. *Acta Acustica united with Acustica, 100(1)*, pp. 34-45.

Vorländer, M. (2008). *Auralization - Fundamentals of Acoustics, Modelling, Simulation, Algorithms and Acoustic Virtual Reality.* Berlin: Springer.

Wilson, D., Pettit, C., Wayant, N., Nykaza, E., & Armstrong, C. (2017). Multilevel modeling and regression of community annoyance to transportation noise. *Journal of the Acoustical Society of America, 142(5)*, pp. 2905-2918.

World Health Organization (WHO). (2018). *Environmental Noise Guidelines for the European Region.*

Wunderli, J., Zellmann, C., Köpfli, M., Habermacher, M., Schwab, O., Schlatter, F., & Schäffer, B. (2018). sonAIR - a GIS-integrated spectral aircraft noise simulation tool for single flight prediction and noise mapping. *Acta Acustica united with Acustica, 104*, S. 440-451.

Zeller, P. (2012). *Handbuch Fahrzeugakustik—Grundlagen, Auslegung, Berechnung, Versuch; 2nd ed.* . Wiesbaden, Germany: Vieweg Teubner Verlag.

Zellmann, C., Jäger, D., & Schlatter, F. (2018). Model Adjustment and Validation to Account for the Airflow Deflector Retrofit of the A320 Family. *11th European Congress and Exposition on Noise Control Engineering (Euronoise 2018).* Crete.

Zellmann, C., Schäffer, B., Wunderli, J., Isermann, U., & Paschereit, C. (2018). Aircraft noise emission model accounting for aircraft flight parameters. *Journal of Aircraft, 55*, pp. 682-695.